POLITECNICO DI TORINO

Master's Degree in Mechatronic Engineering

Master's Degree Thesis

Hysteresis Motor: Transient-Time Model and Observer

Supervisors

Prof. Nicola AMATI

Prof. Andrea TONOLI

Prof. Renato GALLUZZI

Dr. Salvatore CIRCOSTA

Candidate

Matteo SAVIO

Enrolment: 267991

April 2021

Abstract

The objective of this thesis is to analyse the dynamic behaviour of a hysteresis motor by means of a lumped-parameter model. With the development of such model, a flux observer for sensor-less control of this machine is possible.
Previous works in literature present an innovative model for the motor introducing a transient dynamic equivalent circuit and exploiting the state-space model for a field-oriented control. This work implements a model for a particular hysteresis machine prototype in MATLAB/Simulink.
The model considers the equivalent circuit of the motor, adapted to the structure topology and material properties of a hysteresis motor for water pumping applications in automotive systems.
The rotor material of this motor is studied referring to previous works where the alloy was previously described through the Jiles–Atherton model. In particular, experimental hysteresis loops were fitted by means of frequency dependent complex permeability properties.
Integrating the electrical and the mechanical part of the model is possible to perform some open loop simulations, by varying the input condition, to better understand and evaluate the working point of the motor.
The state-space model, used for designing an observer for the control of the hysteresis motor, is presented considering the fluxes and the input currents as states of the system.
At this point an analysis of the poles allow to stabilize and speed up the Luenberger observer gain matrix L, useful for estimate the magnetic flux direction.
This procedure allows to use a field-oriented control approach and opens up to the possibilities to use this kind of motor in closed loop, thus giving new opportunities for further studies.

Summary

1. Introduction

Nowadays, the technology innovation is looking forward to implementing solutions that will build the basis for the future and one of the main points to focus on is relative to the preservation of the environment, reducing the toxic emissions of infrastructures, transports and services. In this direction the electrical motors are receiving a lot of attention due to the opportunity of reduction of CO_2 emissions thanks to the possibility to recover energy from different sources. In order to optimize and help a wide usage of this kind of motor is necessary to guarantee a high efficiency.

Electrical machines are already used in many different areas thanks to some advantages of structure and working behaviour. One of this is the permanent-magnet machine that presents high-power density, high efficiency and simple construction show some problems of demagnetization of the rotor at high temperature. Another example that finds usage in turbo-compound solution is the asynchronous induction machine but presents problems for high rotor velocity as well. An interesting solution of this limits is presented by the hysteresis motor, in fact thanks to a SMHHs material in the rotor it can reach high velocity of the rotor thanks to its robustness and even reach high temperature, ideal condition for a turbomachine. On the contrary, the low magnetic energy density is a disadvantage that significantly impact on this kind of solutions.

For better understanding and analysing the working principle and behaviour of the hysteresis motor in this work is presented a model that opens up to further studies and solutions.

1.1.Hysteresis motor introduction and working principles

The structure of the motor is composed by a stator and a rotor (figure 1.1). The stator consists of an outer ring from which protrude teethes towards the inside of the structure. These teethes create a series of slots occupied by distributed polyphase coils, power-feeded by alternating current.
The rotor is a disk or a cylinder, composed by semihard magnetic material that presents a high degree of magnetic hysteresis. In fact, the principle of working of the motor exploit the magnetic hysteresis energy wasted that is converted into mechanical energy.
The air gap is the portion of space that is present between the two, stator and rotor. Thanks to the polyphase alternating current is generated a rotating magnetic field by the stator, as an induction motor. The magnetization creates magnetic poles on the rotor, that following the rotating field, pull the rotor. The magnetization is affected by hysteresis phenomena that causes a lag between the rotor magnetic field and the air gap magnetic field (figure 1.2).

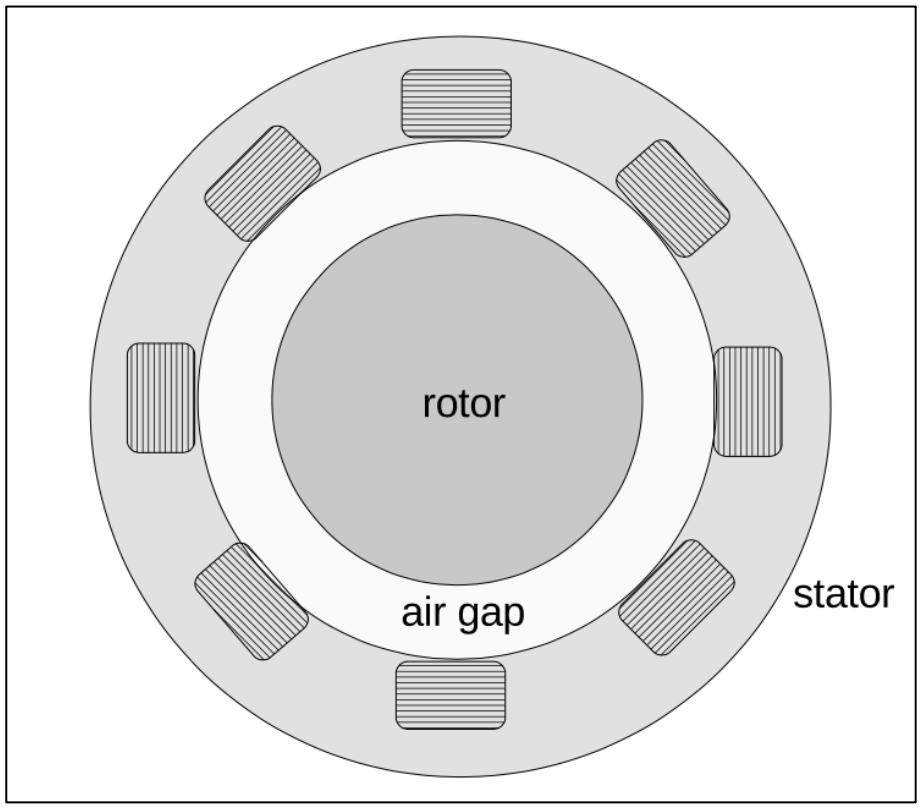

Figure 1.1– *Cross-sectional view of a cylindrical hysteresis motor [1].*

During the first part of the operating state the motor is working asynchronously in the transient, and synchronously at steady state. The ideal hysteresis motor show constant hysteresis torque in transient operation.
The eddy currents effects also contribute to the torque generation when the motor is operating asynchronously. In this phase the motor presents a slip between the stator angular velocity and the rotor one, the stator field interact with the rotor material generating currents that increase the torque due to reduce the slip and obtain a synchronous condition. Eddy currents decrease until the steady conditions are reached.

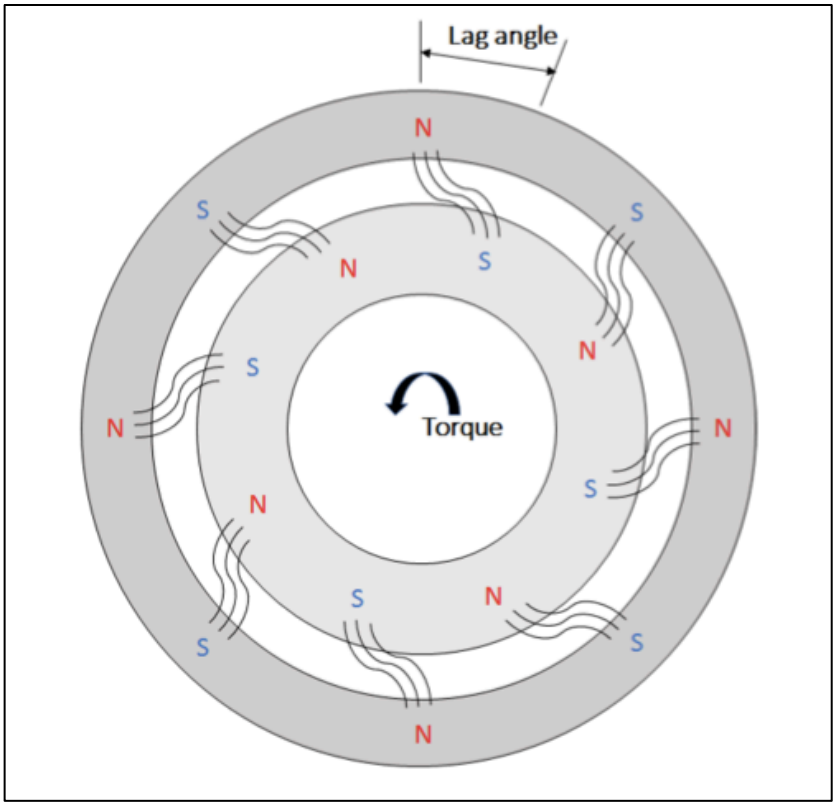

Figure 1.2– *Lag angle.*

Many studies have been done during the years about different model of hysteresis motor [2], also with the introduction of the eddy currents [3]. Here the model is improved thanks to the transformation to quadrature coordinates that imply a remodelling also for the eddy currents.
Another important behaviour that the motor present is the hunting phenomena that rotor have when is lost the asynchronous phase, this aspect is well described by the introduction of working limit given by the lag angle.

As introduced before the hysteresis motor presents some advantages in terms of structure and working mode:

- Smooth and vibration-free thanks to the absence of teeth and windings in the rotor
- Quiet and noiseless
- steady-state speed is directly controlled by the electrical input frequency
- positive starting (non-zero torque at rest)
- no preferential orientation
- constant torque
- moderate current draw during start-up

The main disadvantages are:

- low efficiency
- low power
- hunting phenomena

Due to the absence of vibration and noiseless behaviour of the motor, it finds place in many low power electronic devices for producing or recording sounds and in timing electronic clocks. Mechanical high-speed solution as compressor and pumps are also common, and in fact the motor that has been modelled in this work has been designed and used for a hydraulic pump.

1.2. Structure and objective

The objective of this thesis is to analyse the dynamic behaviour of a hysteresis motor by means of a lumped-parameter model. With the development of such model, a flux observer for sensor-less control of this machine is possible.
In the work are presented the electrical and mechanical relation that involve in the motor and continues with the parameter fitting that better describe the design of the model. Then a MATLAB/Simulink model is presented followed by an analysis of a state-space model for the design of the observer. In the end is calculated the estimated direction of the rotor magnetic flux.

2. Governing equation and equivalent circuits

2.1. Electrical Equations

The analysis of the electrical behaviour of the motor starts from the input voltages and current in the stator coil.
Considering previous studies [1], has been possible to clearly identify the equations that occurs to describe the system.
The motor input is a balanced single-frequency (ω) and three-phase inputs voltage with peak V_0, as equations 2.1 shows:

$$\begin{aligned} v_a(t) &= V_0 \cos(\omega t)\,, \\ v_b(t) &= V_0 \cos\left(\omega t - \frac{2\pi}{3}\right), \\ v_c(t) &= V_0 \cos\left(\omega t + \frac{2\pi}{3}\right). \end{aligned} \qquad 2.1$$

The current follows the voltage input with a phase shift φ and a peak current I_0 :

$$\begin{aligned} i_a(t) &= I_0 \cos(\omega t + \varphi)\,, \\ i_b(t) &= I_0 \cos\left(\omega t - \frac{2\pi}{3} + \varphi\right), \\ i_c(t) &= I_0 \cos\left(\omega t + \frac{2\pi}{3} + \varphi\right). \end{aligned} \qquad 2.2$$

In order to simplify the analysis of the system, the three-phase balanced inputs are transferred to an $\alpha - \beta$ reference system through a transformation matrix T_0.

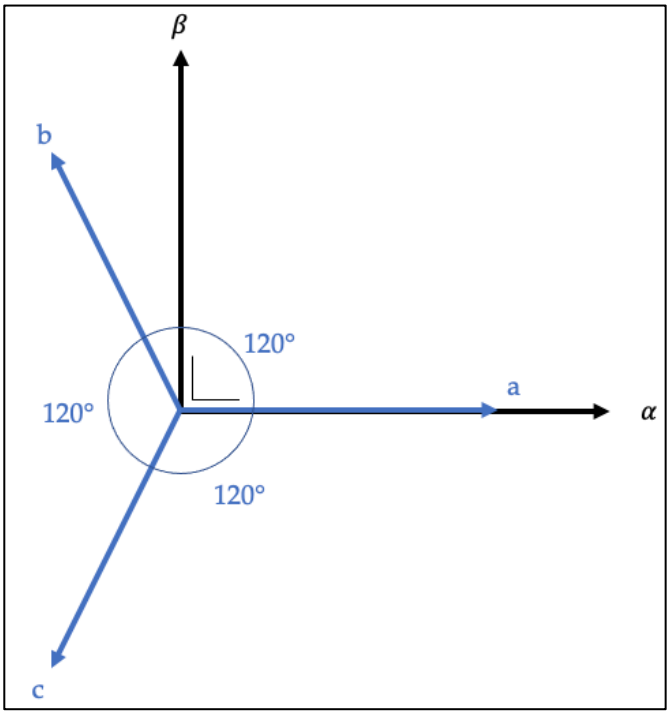

Figure 2.1– *Reference frame transformation.*

The number of solutions variables is reduced from six to four:

$$\begin{bmatrix} v_\alpha \\ v_\beta \\ v_0 \end{bmatrix} = T_0 \begin{bmatrix} v_a \\ v_b \\ v_c \end{bmatrix}, \tag{2.3}$$

$$\begin{bmatrix} i_\alpha \\ i_\beta \\ i_0 \end{bmatrix} = T_0 \begin{bmatrix} i_a \\ i_b \\ i_c \end{bmatrix}, \tag{2.4}$$

$$T_0 = \frac{2}{3}\begin{bmatrix} 1 & -1/2 & -1/2 \\ 0 & -\sqrt{3}/2 & \sqrt{3}/2 \\ 1/\sqrt{2} & 1/\sqrt{2} & 1/\sqrt{2} \end{bmatrix}. \tag{2.5}$$

With a balanced input in 2.1 and 2.2, after the transformation the variables i_0 and v_0 are equal to zero.

Considering the stationary reference frame $\alpha - \beta$ the system is described by equations that take into account the resistances of the stator coil (R_s) and the magnetic fluxes variations ($d\lambda_{\alpha s}, d\lambda_{\beta s}$).

$$v_{s\alpha} = R_s i_{\alpha s} + \frac{d\lambda_{\alpha s}}{dt}, \qquad v_{s\beta} = R_s i_{\beta s} + \frac{d\lambda_{\beta s}}{dt}. \tag{2.6}$$

The equivalent circuit is composed by four different sections that describes the physical behaviour of the motor:

- The stator coil is presented with a resistance R_s and an inductor L_{ls}
- L_m that represent the mutual inductance between stator and rotor
- The hysteresis loop that describes the behaviour of the magnetization in the rotor
- The eddy current in the rotor represented with a resistance R_{Er} and an inductor L_{lEr}

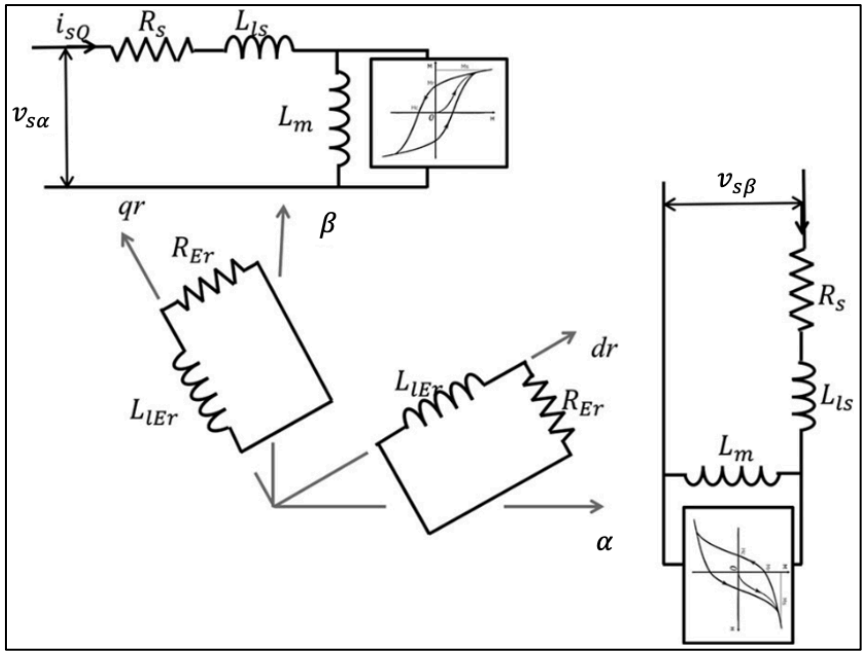

Figure 2.2 – *Rotating frame [4].*

Hysteresis loops present a strong non-linearity in the system and for this reason, in order to obtain a linear working model, an approximation is needed. In this case the hysteresis behaviour between B-H field is approximated to an ellipse, where are considered the maximum magnetization amplitude of the flux density B_m, the magnetic permeability μ and the lag angle δ.
In the equivalent circuits the hysteresis and eddy current behaviour is expressed as follows:

$$0_{2x1} = v_{Hr} = R_{Hr} i_{Hr} + \frac{d\lambda_{Hr}}{dt}, \qquad 0_{2x1} = v_{Er} = R_{Er} i^{r}{}_{Er} + \frac{d\lambda^{r}{}_{Er}}{dt}. \tag{2.7}$$

where R_{Hr} represent the hysteresis resistor, $d\lambda_{Hr}$ the hysteresis flux variation, R_{Er} the eddy current resistor and $d\lambda_{Er}$ the eddy current flux variation.
For what concern the eddy current a transformation (2.8) is needed to represent its behaviour in the stationary reference frame.

$$T = \begin{bmatrix} \cos(\omega_{r,e} t) & -sin(\omega_{r,e} t) \\ sin(\omega_{r,e} t) & \cos(\omega_{r,e} t) \end{bmatrix},$$

$$\frac{d}{dt}\begin{bmatrix} \lambda_{Er,\alpha} \\ \lambda_{Er,\beta} \end{bmatrix} = T \frac{d}{dt}\begin{bmatrix} \lambda_{Er,d} \\ \lambda_{Er,q} \end{bmatrix} + \omega_r T' \begin{bmatrix} \lambda_{Er,\alpha} \\ \lambda_{Er,\beta} \end{bmatrix}, \tag{2.8}$$

$$\frac{d}{dt}\begin{bmatrix} \lambda_{Er,\alpha} \\ \lambda_{Er,\beta} \end{bmatrix} = -\begin{bmatrix} R_{Er} & 0 \\ 0 & R_{Er} \end{bmatrix}\begin{bmatrix} i_{Er,\alpha} \\ i_{Er,\beta} \end{bmatrix} - \omega_r \begin{bmatrix} -\lambda_{Er,\beta} \\ \lambda_{Er,\alpha} \end{bmatrix}.$$

Matrix T is the rotational transformation matrix and in this case the rotation angle in expressed by the terms $\omega_{r,e}$, that is the electrical rotor angular velocity. Is demonstrated in equation 2.8 that is needed a rotational term that cross the flux along α axis and β axis.

In figure 2.3 is presented the whole equivalent circuit with all the component previously described and the adaptation of the eddy current on the stationary reference frame.
In the scheme is evident that a specific equivalent model describes the operating variables of currents and voltages along α and β axle. The terms $\lambda_{Er,\alpha}$ and $\lambda_{Er,\beta}$ are obtained from the eddy current on each axle and introduced in the model.

$$\lambda_{Er,\alpha} = L_m i_{m,\alpha} + L_{lEr} i_{Er,\alpha},$$
$$\lambda_{Er,\beta} = L_m i_{m,\beta} + L_{lEr} i_{Er,\beta}. \qquad 2.9$$

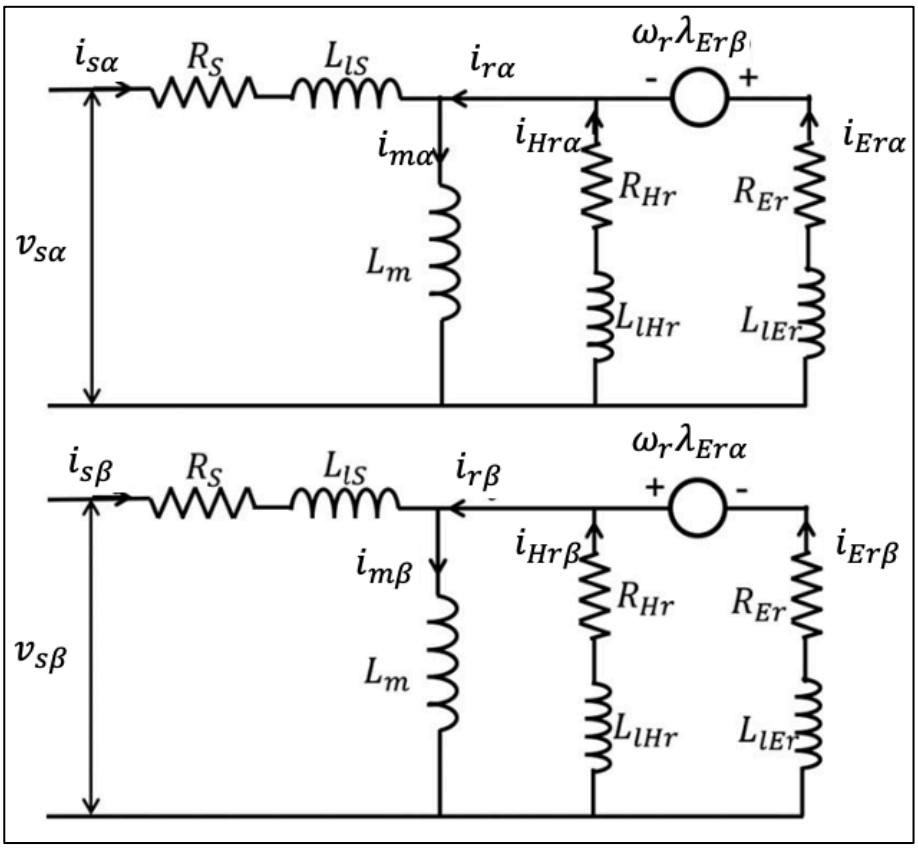

Figure 2.3 - *Equivalent circuit [4].*

The hysteresis behaviour that will be described in chapter 3 originates from the magnetic fluxes $\lambda_{Hr,\alpha}$ and $\lambda_{Hr,\beta}$ that represent the component along the α and β axle derived by the current that flows in the circuits.

$$\lambda_{Hr,\alpha} = L_m i_{m,\alpha} + L_{lHr} i_{Hr,\alpha},$$
$$\lambda_{Hr,\beta} = L_m i_{m,\beta} + L_{lHr} i_{Hr,\beta}. \qquad 2.10$$

From 2.9 and 2.10 it's possible to obtain the total rotor flux λ_r:

$$\lambda_r = \lambda_{Hr} + \lambda_{Er} - L_m i_m , \qquad 2.11$$

with

$$\lambda_r = \begin{bmatrix} \lambda_{r,\alpha} \\ \lambda_{r,\beta} \end{bmatrix},$$
$$\lambda_{Er} = \begin{bmatrix} \lambda_{Er,\alpha} \\ \lambda_{Er,\beta} \end{bmatrix}, \qquad 2.12$$
$$\lambda_{Hr} = \begin{bmatrix} \lambda_{Hr,\alpha} \\ \lambda_{Hr,\beta} \end{bmatrix}.$$

2.2. Mechanical Equations

From the motor's model it is possible to compute the output torque generated by a function of the currents, and of the motor parameter:

$$T_m = \left(\frac{m}{2}\right) P L_m I_g I_r \sin\delta. \tag{2.13}$$

In the equation 2.14, m represent the number of phases, P the number of pole pairs, I_r and I_g are respectively the currents on the rotor and the apparent current in the gap that pass through the inductance L_m and δ is the lag angle.

$$I_r = \sqrt{{i_{r,\alpha}}^2 + {i_{r,\beta}}^2}, \qquad I_m = \sqrt{{i_{m,\alpha}}^2 + {i_{m,\beta}}^2}, \tag{2.14}$$

$$i_{\alpha m} = i_{s,\alpha} + i_{r,\alpha}, \qquad i_{\beta m} = i_{s,\beta} + i_{r,\beta}. \tag{2.15}$$

The electrical angular velocity of the rotor $\omega_{r,e}$ is computed using the conservation of angular momentum, considering in the equation the inertia moment J and the torque load applied to the rotor T_L. The mechanical rotor velocity is $\frac{\omega_{r,e}}{p}$.

$$\frac{J}{P}\frac{d\omega_{r,e}}{dt} = (T_e - T_L). \tag{2.16}$$

3. Circuit component and motor parameter

3.1. Topology of rotor and stator

Here is presented the topology and the functional parameter that is considered for the model and for the simulation that is done.

Motor parameter	Value	Unit
Active length	30	Mm
Stator outside diameter	100	mm
Rotor outside diameter	43	mm
Rotor inner diameter	34.4	mm
Air gap length	0.5	mm
Rotor electrical resistivity (FeCrCo 48/5)	0.7	$\mu\Omega$m

Table 1 – *Motor parameters.*

The active length represents the rotor axial length to consider for the calculation of the circuit's parameters. The air gap is the radial distance between the external circumference of the rotor and the internal circumference of the stator. The motor that we are going to consider is built with one winding made of four coils for each phase, each coil is composed by 9 turns. Conductors of 0,5 mm of diameter organized in parallel shape each turns. Coils for each phase are firstly star linked and then in series.

3.2.Definition of circuit component

The model of the whole system needs to be designed in order to refers to the topology and the materials that represent in the best way the physical behaviour of the motor.

The resistor R_{Hr} is dependant from different factors: input frequency ω_s, the hysteresis parameter μ and δ, and from the topology and winding parameter.

The mutual inductance L_m is described by the magnetic permeability in vacuum considering its influence in the air gap and from the geometry of the section.

L_{Hr} as the resistor R_{Hr} depend on the rotor material hysteresis derived by the parameters μ and δ.

The eddy current resistor R_{Er} is related to the input frequency ω_s in fact increasing the rotor angular velocity is reduced the section for the flow of the eddy current.

Here are presented the inductances and resistors described before in the equivalent circuits [4] [5] [6]:

$$\boldsymbol{R_{Hr}} = \frac{\omega_s m {K_\omega}^2 {N_\omega}^2 V_r \mu}{\pi^2 {r_r}^2} sin\delta, \qquad 3.1$$

$$\boldsymbol{L_m} = \frac{2m{K_\omega}^2{N_\omega}^2\mu_0 r_g l}{\pi p^2 l_g}, \qquad 3.2$$

$$\boldsymbol{L_{Hr}} = \frac{m{K_\omega}^2{N_\omega}^2 V_r \mu}{\pi^2 {r_r}^2} cos\delta, \qquad 3.3$$

$$\boldsymbol{R_{Er}} = \frac{\omega_s \rho l}{5A_h}. \qquad 3.4$$

The variables used are:

- $\boldsymbol{m}$ number of phases
- $\boldsymbol{p}$ number of pole pairs
- $\boldsymbol{K_\omega}$ winding coefficient
- $\boldsymbol{N_\omega}$ number of stators winding per phase
- $\boldsymbol{r_g}$ mean radius of air gap
- $\boldsymbol{l}$ axial thickness of rotor (active length)
- $\boldsymbol{l_g}$ air gap width
- $\boldsymbol{r_r}$ mean radius of rotor ring
- $\boldsymbol{V_r}$ volume of rotor ring
- $\boldsymbol{t_r}$ thickness of rotor ring
- $\boldsymbol{A_h}$ rotor cross-section area
- $\boldsymbol{\rho}$ rotor electrical resistivity

All these parameters referred to the motor under observation are reported in the table below.

Parameter	Value	Unit
m	3	-
p	2	-
K_ω	0,96	-
N_ω	36	-
r_g	21,8	mm
r_r	19,4	mm
V_r	15.684	mm^3
t_r	4,3	mm
A_h	522,79	mm^2

Table 2 – *Parameter for circuits component.*

Considering equation from 3.1 to 3.4 are there two parameters, the lag angle δ and the permeability μ, that are affected by hysteresis magnetization of the rotor and has to be designed in a different way in order to linearize their behaviour. For this reason, an analysis about the material of the rotor and his behaviour under certain input condition is needed.

3.3. Lag angle and permeability

A physical description of the lag angle defines it as the difference between the rotating magnetic field and the magnetized poles on the rotor. Considering instead the lag angle from a cinematic point of view, it can be expressed starting from electrical angular velocity ($\omega_{r,e} = {}^{\omega_r}/_{2}$) as in the following equation:

$$\frac{d\delta}{dt} = \omega_s - \omega_{r,e}. \tag{3.5}$$

Analysing the effective running of the motor during the first phase of sub-synchronism, δ in the model need to be saturate to a value δ_{max} that approximate in the best way the physical working.
When the synchronism is reached, the lag angle starts oscillating about the equilibrium point, giving rise to hunting phenomenon.
For this model an elliptical approximation of the hysteresis loop of the rotor material is used, and for this reason linear resistance and inductor can be introduced in the model.

$$B = B_m \cos\theta,$$
$$H = \frac{B_m}{\mu}\cos(\theta + \delta). \tag{3.6}$$

Equation 3.6 describe the elliptical shape of the B-H curve, with the variables δ and μ that assumes different value depending on the operation point of the motor.
Starting from a previous work [7], where the rotor material of FeCrCo 45/5 is described through the vector generalization of the Jiles–Atherton model and validated through specific simulation of excitation, it's possible to obtain the hysteresis loop of the material under different magnetization field.

In particular the model presents a magnetization vector M derived by:

$$\frac{dM}{dt} = c * \frac{dM_a}{dt} + (I - c)\frac{dM_i}{dt},$$

$$H = \frac{1}{\mu_0}B - M. \qquad 3.7$$

M_a and M_i represent respectively the anhysteretic and the irreversible magnetization terms, c is a reversible tensor. The Langevin function describe the anhysteretic behaviour for the ith terms:

$$M_{a,i} = M_{s,i}\left(\coth\left(\frac{|H_e|}{a_i}\right) - \frac{a_i}{|H_e|}\right)\frac{H_{e,i}}{|H_e|}. \qquad 3.8$$

H_e is the effective magnetic field:

$$H_e = H + \alpha M, \qquad 3.9$$

with α being the interdomain coupling tensor.
The irreversible magnetization is described by a non-liner function:

$$\frac{dM_i}{dt} = \left[(k^{-1}c^{-1}M_r)\frac{dH_e}{dt}\right]^{+}\frac{k^{-1}c^{-1}M_r}{|k^{-1}c^{-1}M_r|}, \qquad 3.10$$

where k represents the pinning tensor.

The reversible magnetization vector is:

$$M_r = c(c - I)^{-1}(M - M_a) \qquad 3.11$$

After a simulation phase through vibrating sample magnetometer, is obtained hysteresis loops for radial and tangential axis. The experimental data were exploited for fitting the model parameter M_s, a, k, c, α, and shows in the tangential axes a higher performance direction of magnetization caused by the anisotropy of the material.
The Jiles-Atherton model for the FeCrCo 48/5 hysteresis loops in the following analysis exploit the parameter obtained for the tangential axes.

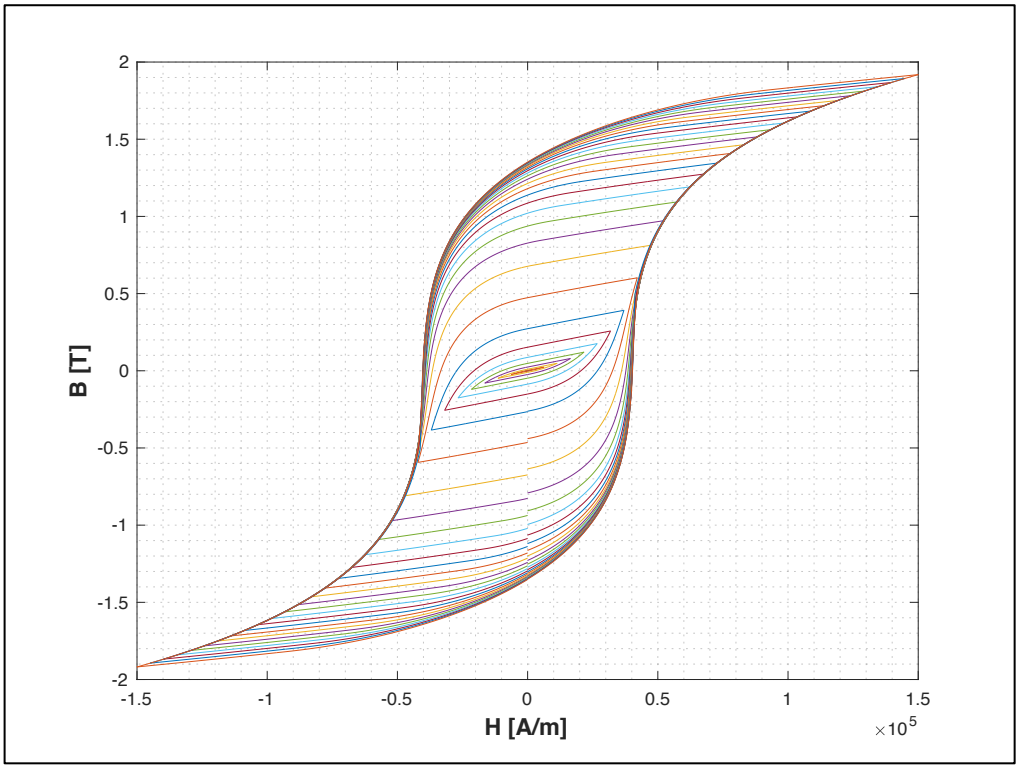

Figure 3.1 – *Hysteresis loops.*

Taking advantage on this accurate study about the rotor material, is possible to generate two lookup table (figure 3.2 and figure 3.3), one for the lag angle and one for the permeability, that best approximate the ellipse on the hysteresis

loops. The approximation is computed in order to reduce the differences of area in the B-H curve.

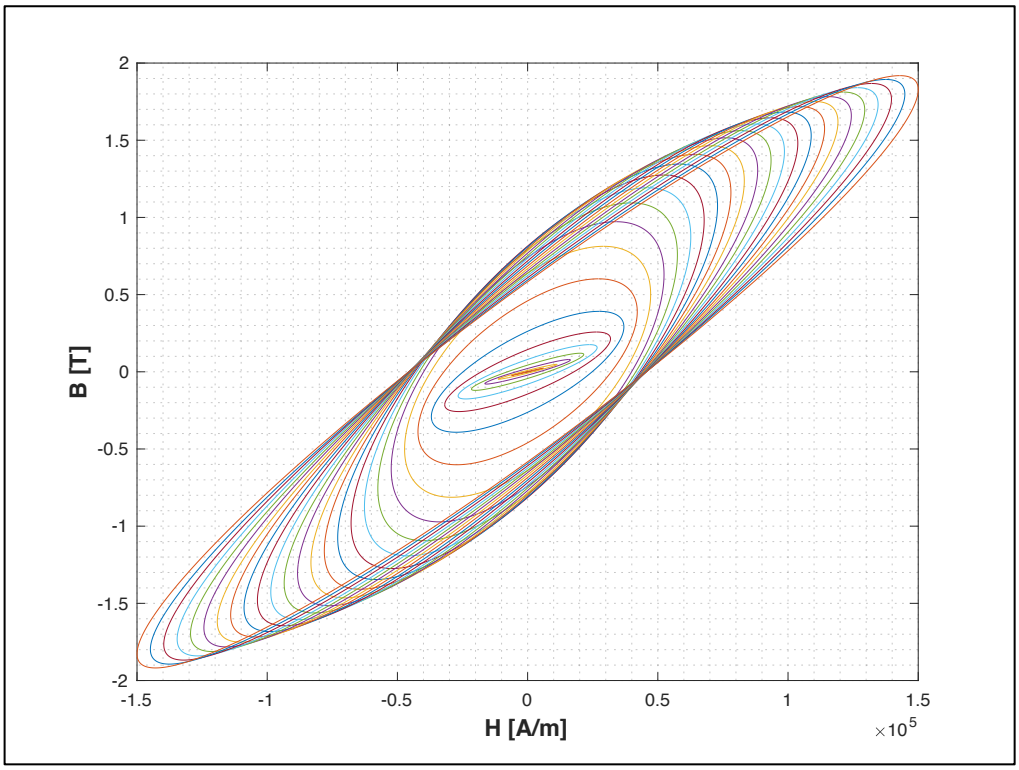

Figure 3.4 – *Hysteresis loops approximation to ellipses.*

The magnetic saturation can be modelled by making the parameters δ and μ as function of the excitation amplitude. In particular is obtained the magnetic flux λ_{Hr} on the rotor and is derived the magnetization field B:

$$B = \frac{\lambda_{Hr}}{N_\omega A},$$

$$\lambda_{Hr} = i_{Hr} L_{Hr}, \qquad 3.12$$

$$A = l * tr.$$

N_ω is the number of windings per phase.

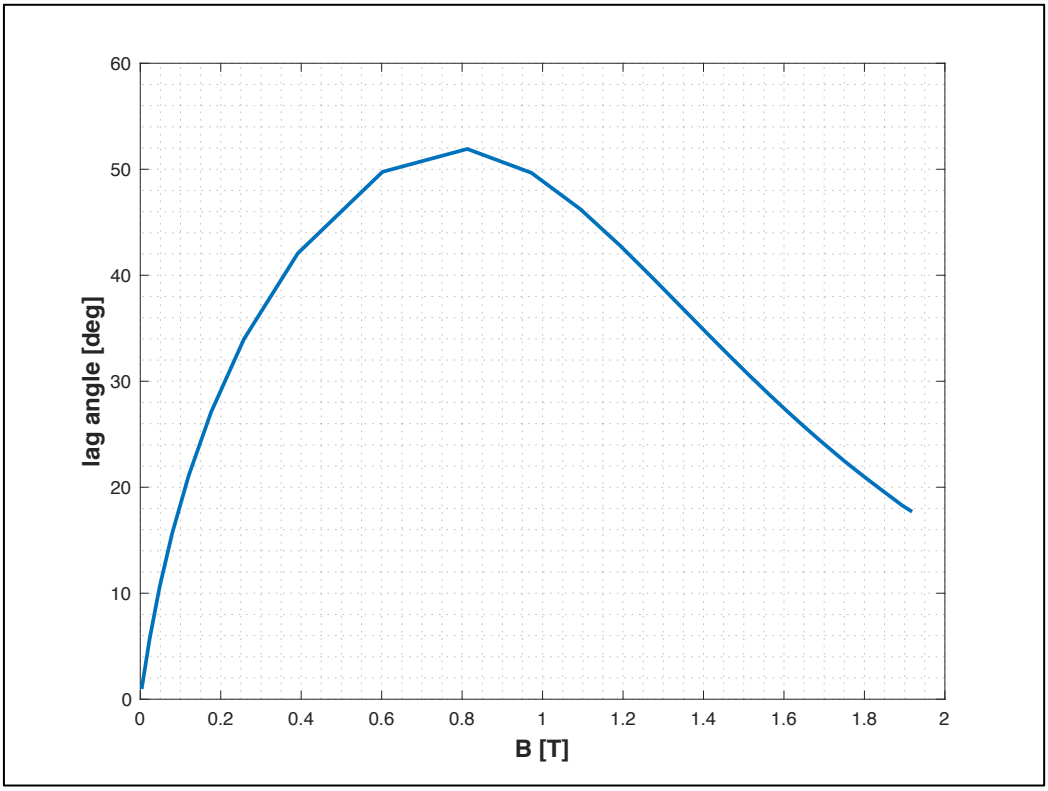

Figure 3.5 – *Lookup table for lag angle.*

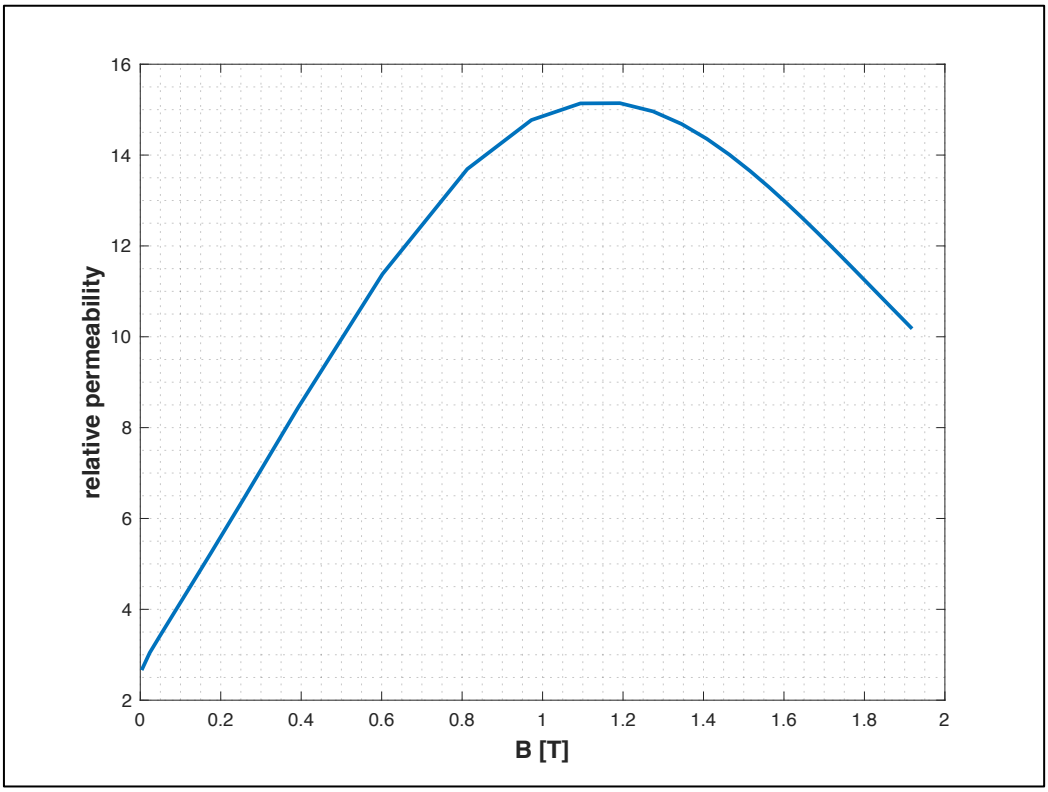

Figure 3.6 – *Lookup table for relative permeability.*

4. Hysteresis motor model

4.1. Simulink model

The model described until now is designed and simulated through MATLAB and Simulink.

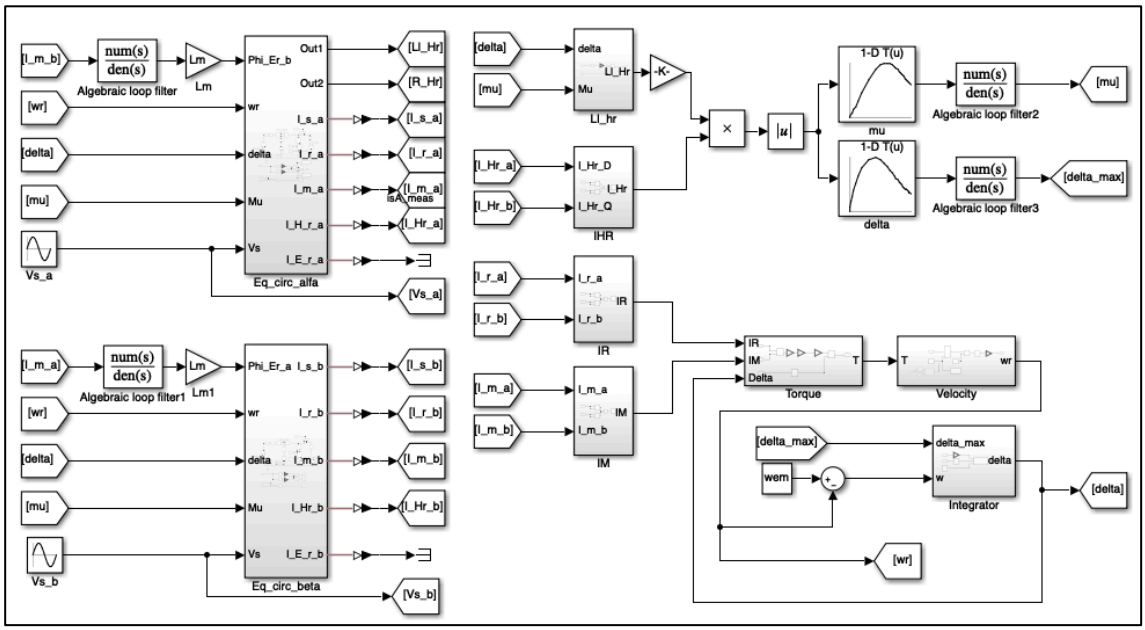

Figure 4.1 – *Whole Simulink model.*

In figure 4.1 is presented the whole system divided into three main part:

- The equivalent circuits
- The hysteresis approximation of the rotor
- The mechanical part

The equivalent circuit are divided between the $\alpha - \beta$ reference frame and are power-feeded by two sinusoidal input current shifted by $\pi/2$.
The input signals of this blocks are:

- The two parameters δ and μ from the lookup table
- The rotor electrical angular velocity $\omega_{r,e}$
- The currents $i_{m,\alpha}$ and $i_{m,\beta}$ respectively in the β and α circuits

In particular from the δ and μ are derived the two hysteresis approximation parameters R_{Hr} and L_{Hr}. Referring to 2.8, currents are used for evaluating the

mutual flux linkage from which is derived the voltage generator for modelling the eddy currents on the stator reference frame.
The output of this blocks are all the currents that flow through the circuits.

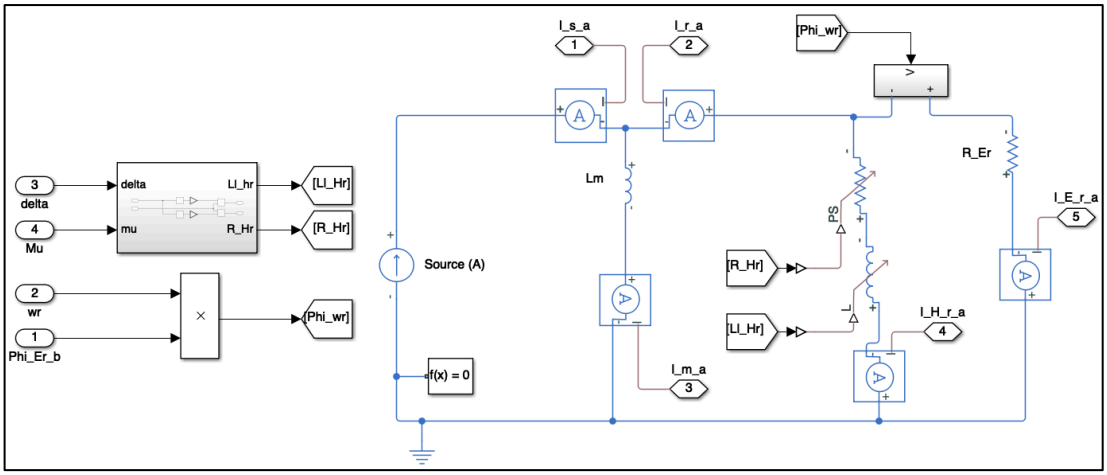

Figure 4.2 – *Equivalent circuit: α reference frame.*

Exploiting the currents $i_{Hr,\alpha}$ and $i_{Hr,\beta}$, it's possible, as described in 3.6, to obtain the flux and the magnetic field intensity for evaluating the parameters δ and μ through the lookup table described in the previous chapter.
The δ obtained through this process is considered as a limit saturation of the lag angle due to the rotor limit magnetization, and for this reason is stored as δ_{max}.

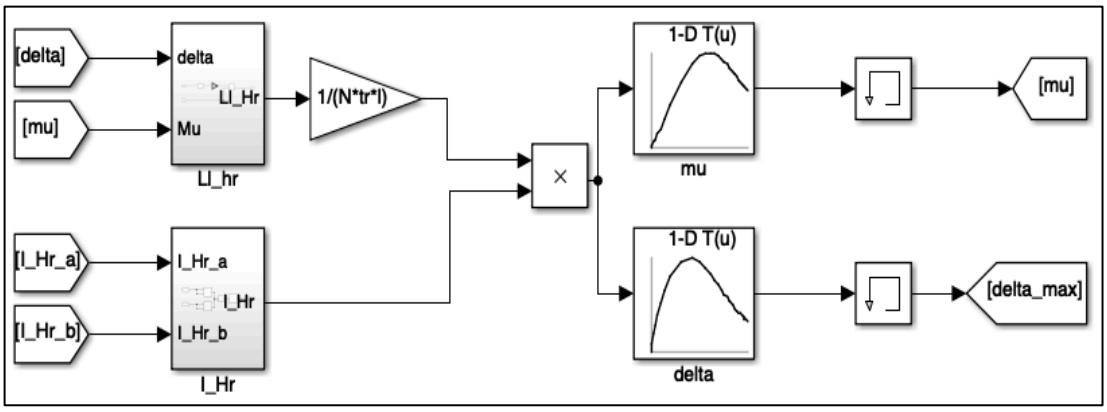

Figure 4.3 – *Parameters δ and μ.*

For what concern the mechanical part the equation from 2.11 to 2.14 are introduced in the model. Is calculated the torque generated by the motor by means of the currents, the mutual inductance L_m and the lag angle δ. For modelling the dynamics of the system in the simulation is introduced a frictional resistant torque.

The lag angle is the parameter that, as described in 3.5, from a cinematic point of view, allow to reach the synchronism.

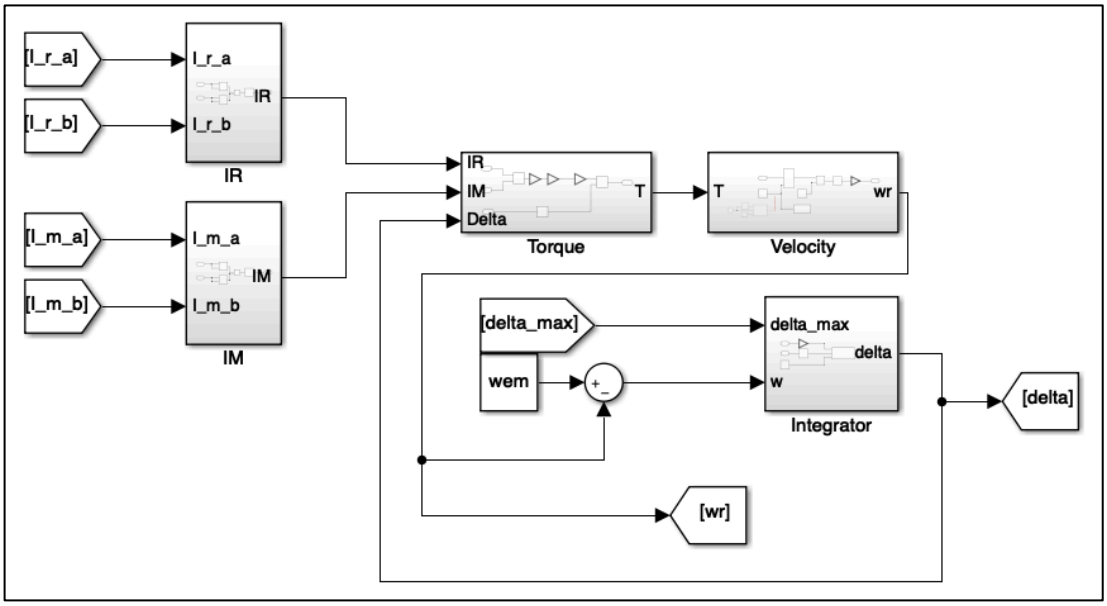

Figure 4.4 – *Mechanical model.*

4.2. Open loop simulation

For evaluate the whole model some open loop simulations are performed.
The inputs of the system are the voltages on the stator implemented on the α and β axle. For simplicity and for link the results with the previous work [7] of this motor, is considered the input current density with its frequency.

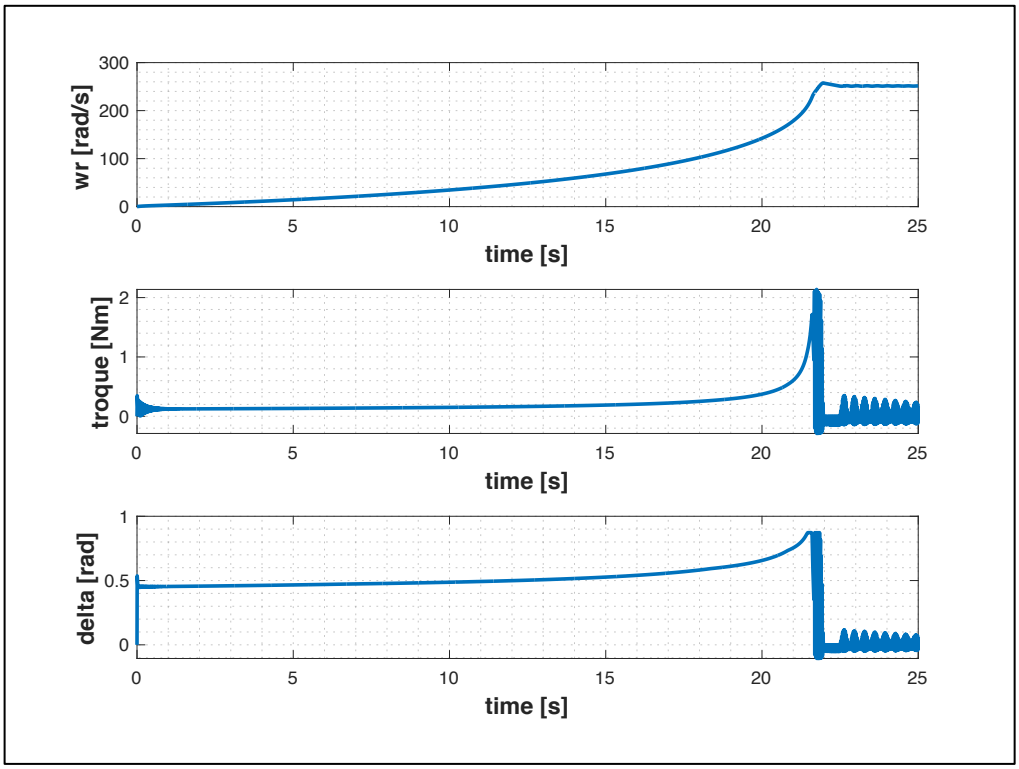

Figure 4.5 – *Simulations 2,5 A/mm^2 80 Hz.*

The first plot in figure 4.5 shows the behaviour of the angular velocity of the rotor during the simulation time, the rotor speed increment until the synchronism is reached and from this point forward it starts oscillating generating the hunting phenomena.
The delta angle expressed in radians assumes an initial value, that is limited by δ_{max} in order to follow the saturation limit of the rotor and start oscillating when the rotor reaches the synchronism.

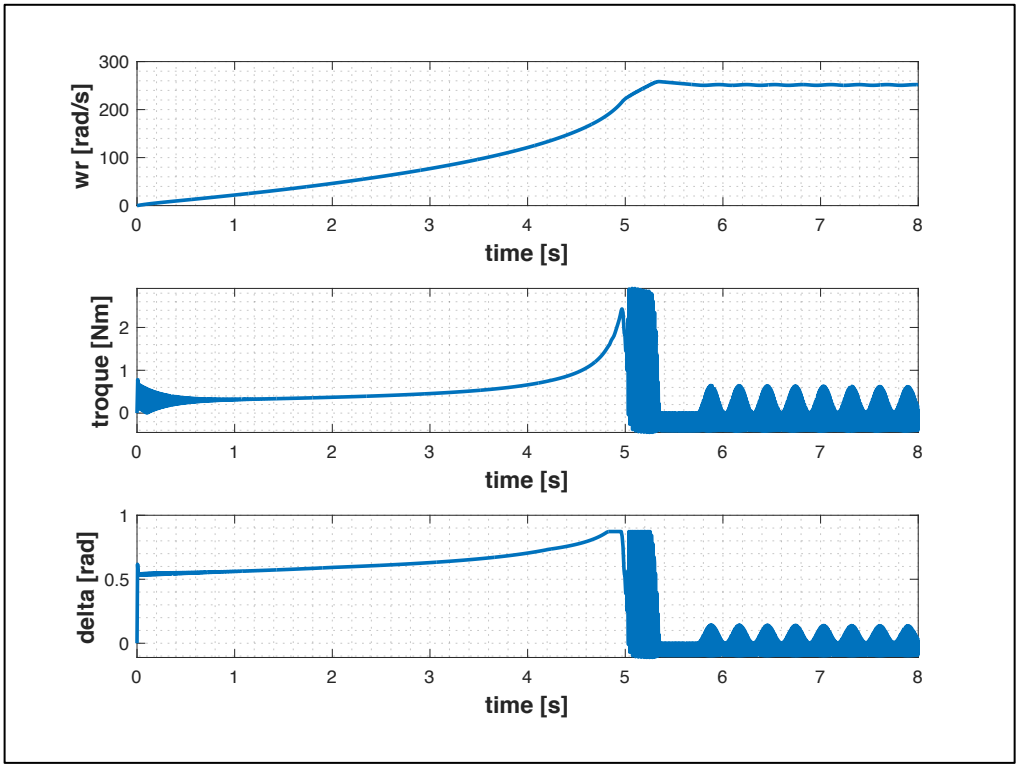

Figure 4.6 - *Simulations 3,5 A/mm² 80 Hz.*

From the figure 4.6 is well evident the different behaviour of the plotted parameter against the first simulation in figure 4.5. With an input current higher, increase the torque of the motor that affect the acceleration and synchronism arrive earlier.

In the simulation of figure 4.7 is reduced to 50 Hz the frequency of the stator's current and the rotor angular velocity reaches the synchronism at lower speed.

In figure 4.8 increasing the input frequency to 100 Hz shows the possibility of evaluate the model working under different input conditions.

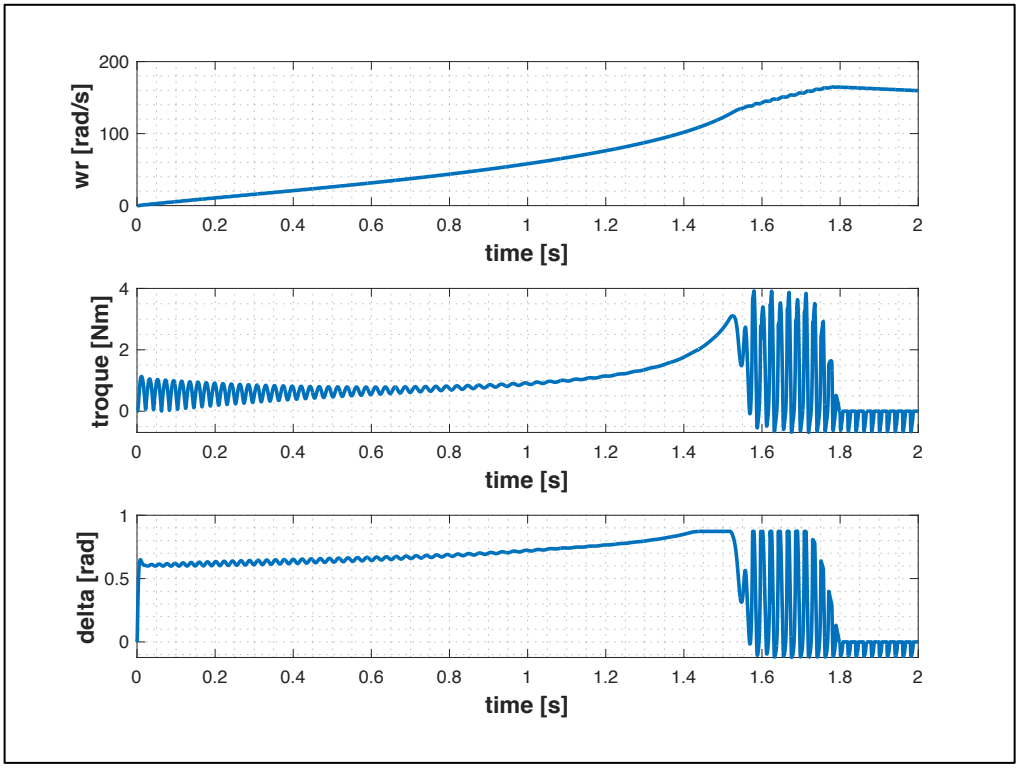

Figure 4.7 - *Simulations 3,5 A/mm² 50 Hz.*

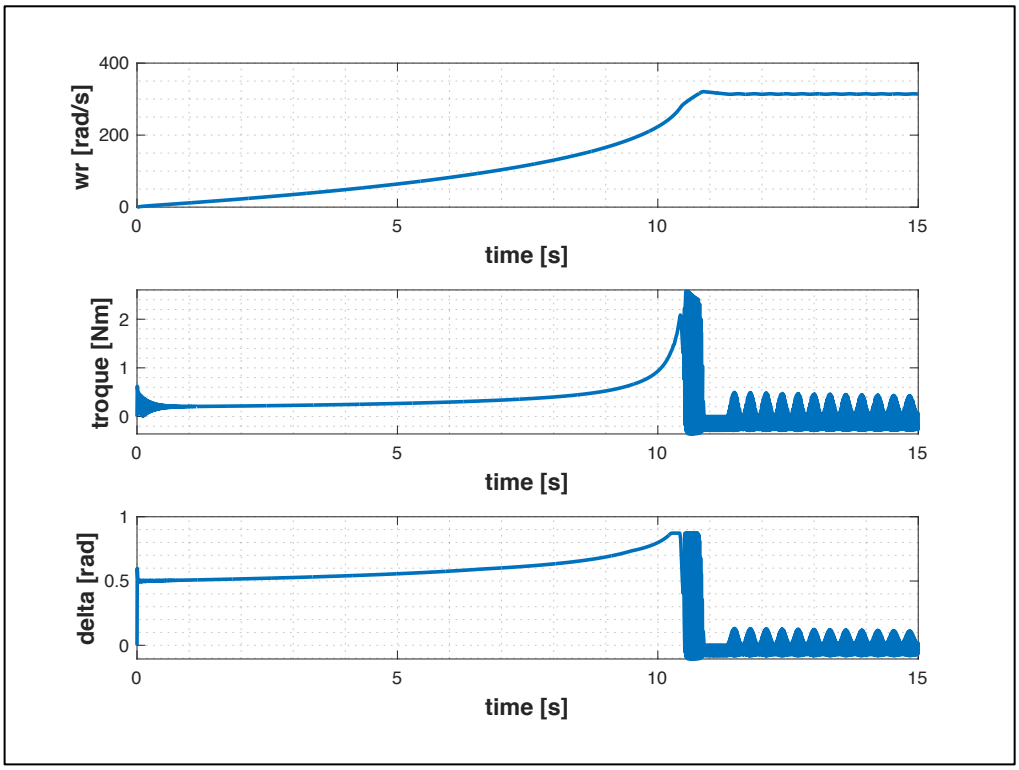

Figure 4.8 - *Simulations 3,5 A/mm² 100 Hz.*

5. State-space model and observer

From the equivalent circuit in transient time described in the stationary frame $\alpha-\beta$, it is possible to obtain the state space model useful for the implementation of the observer and of the control.
The three states considered are the current on the stator i_s, and the two fluxes generated due to hysteresis (λ_{Hr}) and eddy currents (λ_{Er}).

$$\begin{aligned} i_s &= [i_{s,\alpha}\ i_{s,\beta}]^T, \\ \lambda_{Hr} &= [\lambda_{Hr,\alpha}\ \lambda_{Hr,\beta}]^T, \\ \lambda_{Er} &= [\lambda_{Er,\alpha}\ \lambda_{Er,\beta}]^T. \end{aligned} \qquad 5.1$$

Useful for the state-space model description are the matrix I, J and Z expressed as below:

$$\begin{aligned} I &= \begin{bmatrix} 1 & 0 \\ 0 & 1 \end{bmatrix}, \\ J &= \begin{bmatrix} 0 & -1 \\ 1 & 0 \end{bmatrix}, \\ Z &= \begin{bmatrix} 0 & 0 \\ 0 & 0 \end{bmatrix}. \end{aligned} \qquad 5.2$$

Considering the three state of the model the state-space can be described by the matrix A, B, C and D.

$$\begin{aligned} \dot{x} &= Ax + Bu, \\ y &= Cx + D, \end{aligned} \qquad 5.3$$

$$i_s = [I\ Z\ Z] \begin{bmatrix} i_s \\ \lambda_{Hr} \\ \lambda_{Er} \end{bmatrix}, \qquad 5.4$$

$$\frac{d}{dt}\begin{bmatrix} i_s \\ \lambda_{Hr} \\ \lambda_{Er} \end{bmatrix} = \begin{bmatrix} -\gamma I & \alpha I & \beta I - \dfrac{\sigma L_m L_{lHr}\omega_r}{\kappa} \\ \sigma R_{Hr} L_m L_{lEr} I & -\sigma R_{Hr} L_{lEr} I & \sigma L_m R_{Hr} I \\ \sigma R_{Hr} L_m L_{lHr} I & \sigma L_m R_{Er} I & -\sigma R_{Er} L_{Hr} I + \omega_r J \end{bmatrix} \begin{bmatrix} i_s \\ \lambda_{Hr} \\ \lambda_{Er} \end{bmatrix} + \begin{bmatrix} \dfrac{1}{\kappa} I \\ 0 \\ 0 \end{bmatrix} v_{s.} \qquad 5.5$$

In the equations are introduced the values of the resistor and of the inductance presented in the chapter 2 and are introduced L_s, L_{Er}, L_{Hr} that are respectively:

$$\begin{aligned} L_s &= L_m + L_{ls}, \\ L_{Er} &= L_m + L_{lEr}, \\ L_{Hr} &= L_m + L_{lHr}. \end{aligned} \qquad 5.6$$

The other parameters are defined by,

$$\begin{aligned} \sigma &= 1/(L_{Hr}L_{Er} - {L_m}^2), \\ \kappa &= L_s - \sigma {L_m}^2 (L_{lEr} + L_{lHr}), \\ \gamma &= (R_s + \sigma^2 {L_m}^2 ({L_{lEr}}^2 R_{Hr} + {L_{lHr}}^2 R_{Er}))/\kappa, \\ \beta &= (\sigma^2 L_m (R_{Er} L_{Hr} L_{lHr} - R_{Hr} L_m L_{lEr}))/\kappa. \end{aligned} \qquad 5.7$$

From 5.5 is well evident how the variables of the state-space can be described by the parameters of the circuit but in some cases these parameters are depending by the working point of the motor.

In particular the parameters R_{Hr} and L_{Hr}, considering that its value is characterized by the non-linear hysteresis behaviour described in chapter 3, have to be modelled in order to obtain the matrix to perform the observer and the control.

The other variable to take into account is the rotational velocity of the rotor ω_r, from which depend the whole system.

The model presented in this chapter is used to estimate the rotor flux orientation through a full-order state observer.

Rewriting the system equation as:

$$\dot{x} = Ax + Bv_s, \qquad y = Cx. \tag{5.8}$$

A and B are presented in 5.5, $y = i_s = [i_{s\alpha}, i_{s\beta}]^T$ and $C = [I, Z, Z]$ as in 5.3. A Luenberger observer can be designed as follows:

$$\dot{\hat{x}} = A\hat{x} + Bu + L(y - C\hat{x}), \tag{5.9}$$

whit $\hat{x}$ that is the estimated state, and L is the observer gain matrix.
At this point some simulation is performed in order to evaluate how the matrix A variate during the simulation process.
Due to analyse the variations on the single element of the 6x6 matrix A, some simulations and the matrix composition are useful to detect a relation between the state space matrix and the rotor angular velocity.
Starting with the components A_{16} and A_{56} is evident from equation 5.5 that in both cases it depends on the angular velocity of the rotor, in the first one the dependence is direct, in the second case is inverse.
The parameter related to the hysteresis behaviour (R_{Hr}, L_{Hr}) are strongly dependant by the rotor angular velocity, so the components of the matrix A described by this parameter are influenced by ω_r.
Some other components maintain a constant value during all the simulation.
After the analysis on the matrix component is difficult to obtain a gain scheduling dependent from the parameter of ω_r.

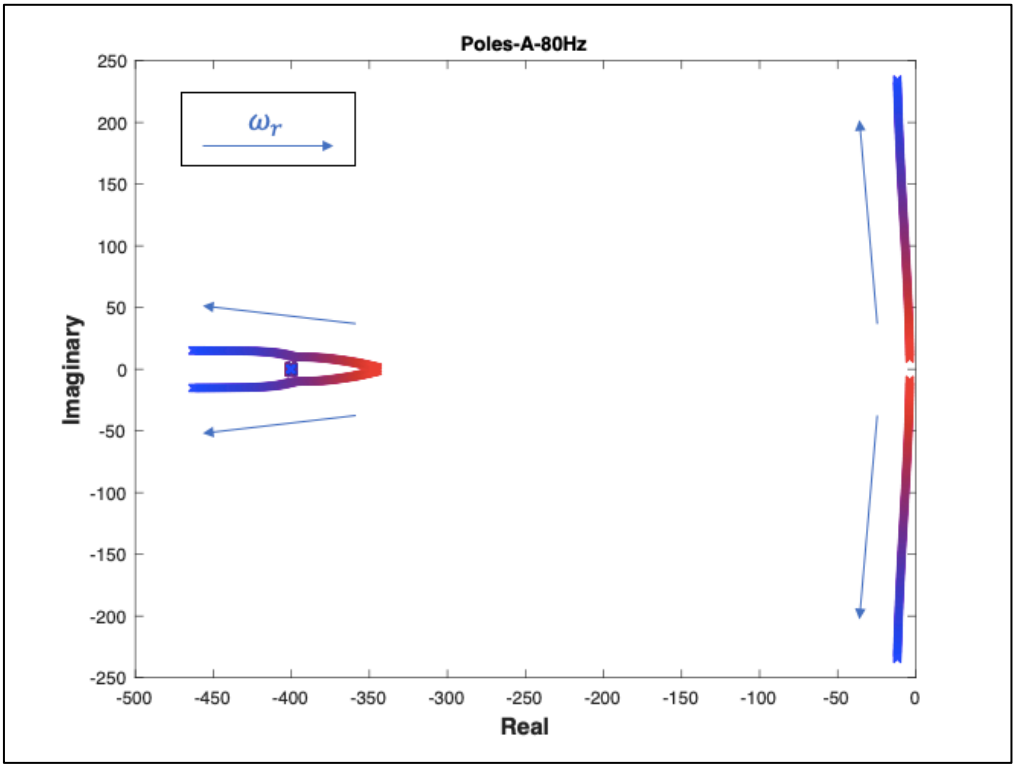

Figure 5.1 – *Eigenvalue of matrix A with input frequency of 80Hz.*

In order to perform a design through pole placement of the gain matrix L, has been analysed a set of matrices A, B, C and D imposing the rotor velocity and obtaining a constant value in the components of the matrix.

Each rotor velocity value has a corresponding set of matrices. This process is computed for each frequency input.

In figure 5.1 are presented the three couples of poles in the imaginary plane of the matrix A with an input frequency of 80Hz and an input current of 3,5 A/mm^2, the colormap starts from low velocity in red until high velocity in blue, that in this case represent the synchronism velocity of 251 rad/s.

Considering the poles of the matrix A, it's possible to evaluate the stability of them and the series of poles near zero with the real part are close to the unstable area of the graph, and for this reason is necessary to find a couple of poles that stabilize the system in order to obtain a suitable observer.

In figure 5.2 are shown in red the couple of poles that has to be modified. The dynamics of the observer is determined by the matrix $A - LC$, so in green are underlined the poles that have to be placed in the system in order to obtain a fast and stable observer.

Considering a damping factor ζ of $\frac{1}{\sqrt{2}}$, the $\cos^{-1}\zeta$ is equal to 45° that is the angle φ represented in figure 5.2 to replace the red couple of poles and maintaining the same distance from the origin.

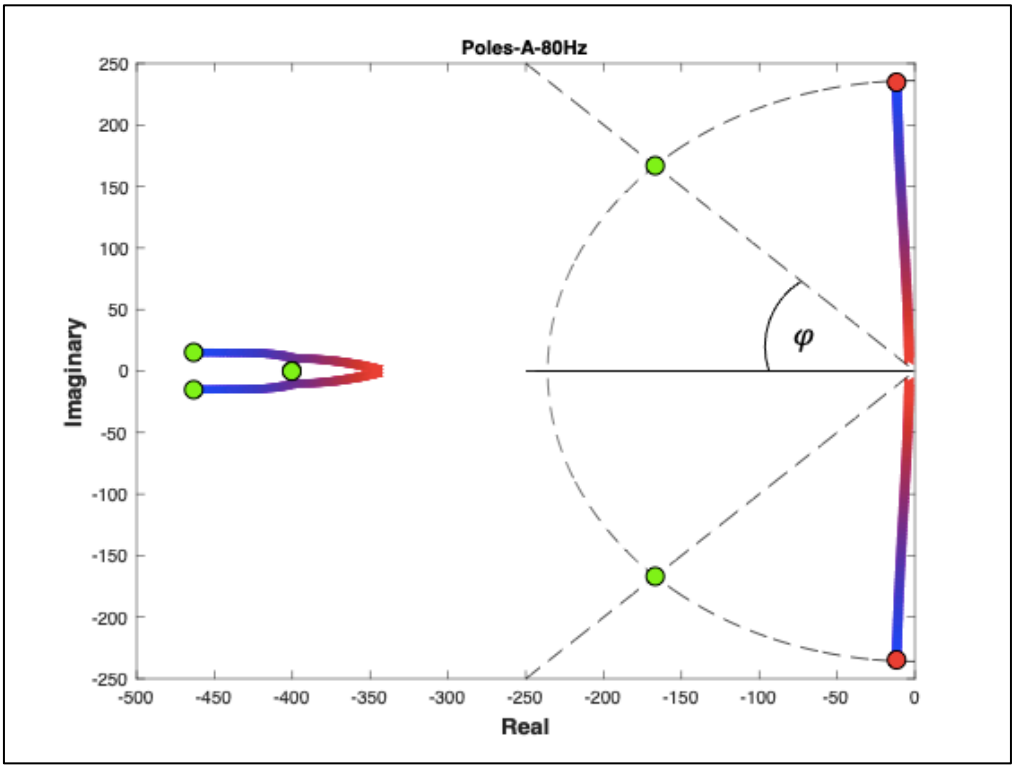

Figure 5.2 – *Pole placement in green.*

The poles in green in figure 5.2 are expressed in the table 3.

-166,87 + 166,87i
-166,87 - 166,87i
-463,38 + 015,18i
-463,38 - 015,18i
-400,38 + 0,12i
-400,38 – 0,12i

Table 3 – *Pole placement*

The model present three states shared for the frame $\alpha - \beta$, for a total of six observed states. In figure 5.3 is presented the current that flows in the stator measured from the model in relation with the current observed, after 0,001 s is enabled the observer and is well evident how it follows the signal that is measured.

The two fluxes λ_{Hr} and λ_{Er} are the states that need for the calculation of the estimated direction of the rotor flux. As described in equation 2.11 ($\lambda_r = \lambda_{Hr} + \lambda_{Er} - L_m i_m$), it is possible to obtain the total flux on the rotor λ_r, and as expressed in equation 5.9, estimate the θ angle that represent the position of the rotor.

$$\sin\hat{\theta} = \frac{\hat{\lambda}_{r,\beta}}{\sqrt{\hat{\lambda}^2{}_{r,\alpha} + \hat{\lambda}^2{}_{r,\beta}}}, \qquad 5.10$$

$$\cos\hat{\theta} = \frac{\hat{\lambda}_{r,\alpha}}{\sqrt{\hat{\lambda}^2{}_{r,\alpha} + \hat{\lambda}^2{}_{r,\beta}}}.$$

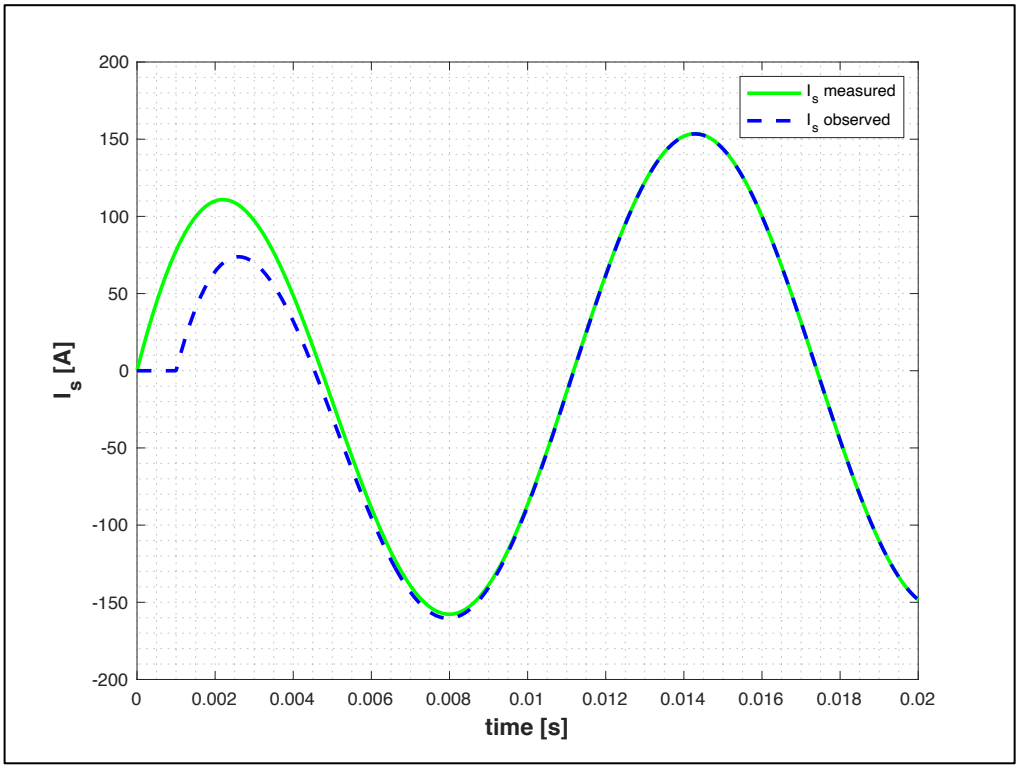

Figure 5.3 – *Check on stator current measured and observed.*

For the figure 5.4 are considered for theta measured the current and the inductor obtained by the model simulation that are previously described in 2.9 and 2.10:

$$\lambda_{Er,\alpha} = L_m i_{m,\alpha} + L_{lEr} i_{Er,\alpha},$$

$$\lambda_{Er,\beta} = L_m i_{m,\beta} + L_{lEr} i_{Er,\beta}. \qquad 5.11$$

$$\lambda_{Hr,\alpha} = L_m i_{m,\alpha} + L_{lHr} i_{Hr,\alpha},$$

$$\lambda_{Hr,\beta} = L_m i_{m,\beta} + L_{lHr} i_{Hr,\beta}. \qquad 5.12$$

Theta estimated is calculated by the flux obtained by the observer. It is possible to evaluate haw after a transient in which the two signals are not in phase, around the time of 0,7 s the estimated value follows the measured one confirming and validating the effective working of the observer.
With this method it is possible to know and estimate the real direction of the flux through a field-oriented approach.

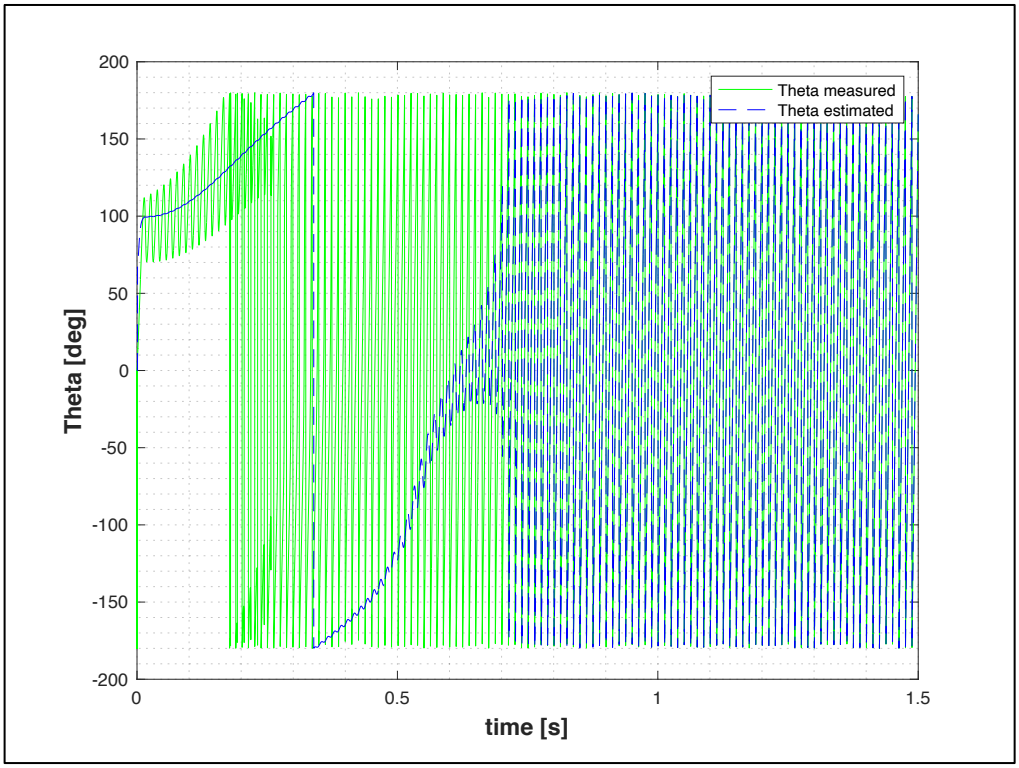

Figure 5.4 – *Theta measured, and theta estimated.*

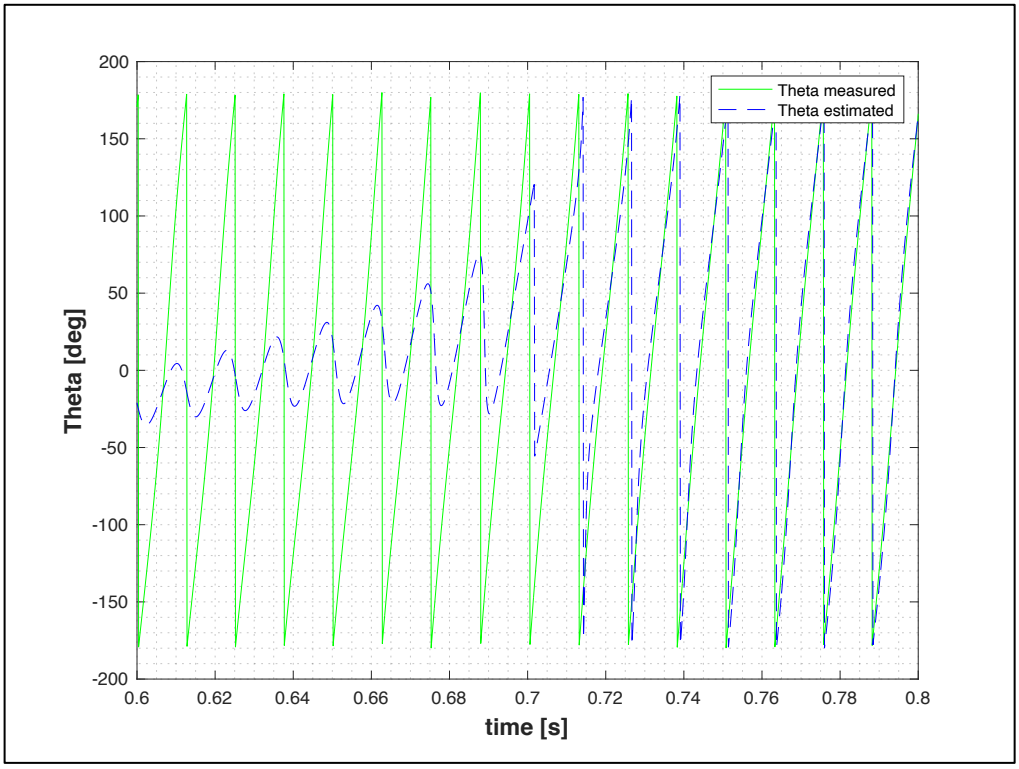

Figure 5.5 – *Theta measured, and theta estimated zoom.*

6. Conclusions

The model designed in the thesis represent a solid basis for evaluating and analysing through different studies possible solution for the hysteresis motor.
Thanks to previous works about the rotor material is described a good approximation of the hysteresis that represent the main obstacle for the linearization of the model.
The transient time behaviour is well described and open to the opportunities of simulating and to collect data under different input signals. It's possible in this way to establish a direct connection with the generated torque or with the angular velocity of the rotor.
Moreover, the model allows to obtain a good vison about the magnetic fluxes generated by the stator that influence the rotor in the rotational mechanism.
The analysis of the state-space model and the design of the observer implemented in the model through field-oriented approach, allow a good estimation of the flux direction and represent a good starting point for a sensor-less control of the motor.
An interesting application for hysteresis motor is presented by the possibility to use this kind of motor in high-speed solution as for example turbo-compressors, with a regenerative brake, in order to exploit the machine as generator. This model is a first step to evaluate the opportunities that this kind of motor can offer.

References

[1] E. S. B. K. J.J. Nitao, “Equivalent Circuit Modeling of Hysteresis Motors,” 2009.

[2] S. M. a. T. Kataoka, ““A basic equivalent circuit of the hysteresis motor”,” 1965.

[3] S. M. a. T. Kataoka, “Analysis of hysteresis motors considering eddy current effect,” 1966.

[4] W. G. D. L. T. Lei Zhou, “Position Control for Hysteresis Motors: A Field-oriented Control Approach,” 2018.

[5] D. Hanselman, Brushless Permanent Magnet Motor Design, 2006.

[6] Ø. K. R. N. S. E. Skaar, “Distribution, coil-span and winding factors for PM machines with concentrated windings,” 2006.

[7] N. A. a. A. T. Renato Galluzzi, “Modeling, Design, and Validation of Magnetic Hysteresis Motors,” 2020.

[8] J. J. N. E. T. S. a. B. A. Kirkendall, “Equivalent Circuit Modeling of Hysteresis Motors,” 2009.